Nanofabrication

DOI: 10.1002/anie.201106490

Facile Fabrication of Metallic Nanostructures by Tunable Cracking and Transfer Printing**

*Juan Zhu, Mianqi Xue, Dan Zhao, Meining Zhang, Lian Duan, Yong Qiu, and Tingbing Cao**

Fabrication of well-ordered metallic nanostructures over large areas has drawn great interest in recent years, owing to their increasing applicability in optoelectronics,[1] chemical sensors and biosensors,[2] and particularly plasmonics such as surface plasmon resonance (SPR)[3] and surface-enhanced Raman scattering (SERS).[4] Owing to the importance of metallic nanostructures, a number of experimental methods have been developed to date to fabricate such surfaces. The most commonly used methods for the micro- and nanofabrication are photolithography[5] and electron-beam writing,[6] but they are often prohibitively expensive, which has limited accessibility for the general users, and they are incompatible with many organic and biologic species, as well as with nonplanar substrates.[7]

Among the emerging unconventional fabrication approaches in recent years, soft lithography[8] shows powerful vitality in preparing micro- and nanostructures. It often employs an elastomeric stamp made of poly(dimethylsiloxane) (PDMS) to transfer patterns by simple molding or printing.[9–11] Organic silanes or thiols,[9,12] biological proteins[13] or DNA molecules,[14] and many other materials normally used in or compatible with electronic devices[10] can be patterned directly through a convenient microcontact printing process. Rogers and co-workers extended the application of soft lithography methods to the patterning of metallic electrodes with two- or three-dimensional structures and named the technique nanotransfer printing (nTP).[11] The nTP technique, which is a very useful novel type of soft lithography, has shown great potential in the manufacturing of flexible electronics and optical devices such as field-effect transistors (FETs),[15] complementary metal oxide semiconductor (CMOS), and optoelectronics containing organic crystals.[16]

Generally, soft lithography can be applied to mold or print different materials with dimensions above sub-micrometer size, since it is difficult for elastomeric PDMS molds to directly generate nanoscale features. Founded on the soft lithography platform, numerous efforts have been explored in fabricating sub-100 nm nanostructures in the presence of edge lithography,[17,18] near-field optical lithography,[19] phase-shifting lithography,[20] and so forth. Recently, the use of thin sectioning or nanoskiving to fabricate nanostructures has been developed by Xu, Whitesides et al., and the method has drawn wide attention for optical and electronic applications, include surface plasmon resonators, plasmonic waveguides, chemoresistive nanowires, and heterostructures of organic semiconductors.[21,22]

Herein, we report an interesting approach in fabricating metallic nanostructures by using a combination of metal thin film deposition, organic-vapor-assisted PDMS stamp swelling, and transfer printing. In comparison with the mechanical stretch of elastomeric stamps, the vapor swelling of PDMS is much easier to operate with fine-tunable or programmable factors by exposing the stamp to different organic vapors.[23] Since metal thin films deposited from the vapor phase are very brittle upon exertion of external force, the swelling of the PDMS stamp beneath will inevitably cause the fracture of the metal film. Herein we investigate the cracking of thin metal films into different metal nanostructures through tuning of the swelling ratio of the PDMS stamp in response to different organic solvents. The facile approach shows great advantages in the nanofabrication after transfer printing of metallic nanostructures on silicon or flexible substrates, even compared with other unconventional methods, including photo-induced deposition, electrochemical roughening, or de-alloying of metal surfaces.[24,25]

Figure 1 shows the procedure to fabricate the metal nanostructures by tunable cracking and transfer printing. Firstly, we have prepared a PDMS stamp with topography preliminarily determined by photolithography. Then a thin film of gold metal is deposited onto the PDMS stamp through magnetic sputtering. The resulting films have thicknesses ranging from several to dozens of nanometers. The PDMS stamp with thin gold film is placed into a sealable chamber, which is filled with saturated organic vapor. After settling for a period of time, the PDMS stamp is gently swelled under the organic vapor, and the metal thin film is cracked into different pieces. Finally, the PDMS stamp with Au film is conformally contacted with a silicon wafer or flexible plastic substrate to which a self-assembled monolayer (SAM) of thiol is attached to peel the Au nanostructures from the PDMS stamp to accomplish the nanotransfer printing process.

Several factors determine the shape and size of as-prepared metallic nanostructures. As shown in Figure 1, the microscopic shape of metal structures is incontestably determined by the PDMS stamp, the same as in typical nTP and other soft lithography process. The organic solvent and vapor can greatly affect the fracture and cracking of metal thin film

[*] J. Zhu, M. Xue, D. Zhao, Prof. M. Zhang, Prof. T. Cao
Department of Chemistry, Renmin University of China
Beijing 100872 (China)
E-mail: tcao@chem.ruc.edu.cn
Dr. L. Duan, Prof. Y. Qiu
Key Lab of Organic Optoelectronics and Molecular Engineering of Ministry of Education
Department of Chemistry, Tsinghua University
Beijing 100084 (China)

[**] This research was supported by the National Science Foundation of China under grant No. 20733001, 91027029.

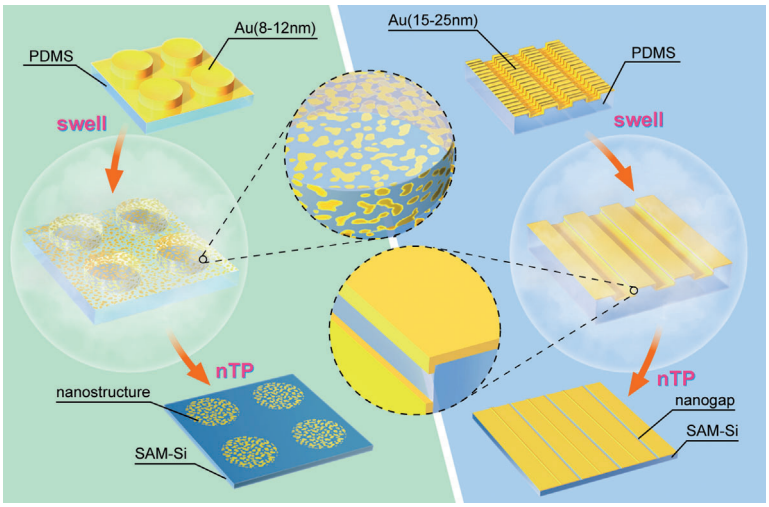

Figure 1. A schematic illustration of the procedure for the fabrication of metal nanostructures by cracking of metal film under organic vapors.

through swelling the PDMS stamp; since PDMS has various swelling ratios under different organic solvents or their mixtures, the cracking and as-transferred metal nanostructures can be finely tuned in the nanoscopic range. Finally, the thickness of the metal film, together with the manner in which the film is deposited, also influence the final nanostructures. The left side of Figure 1 shows the cracking of metal thin film with thickness around 10 nm. The film breaks into nanoparticle shapes upon vapor swelling, which is quite similar to the thermal annealing and dewetting of ultra-thin gold film.[26] After transfer printing, the round the nanoparticle arrays can be fabricated on silicon wafer. The right side of Figure 1 shows tunable cracking of a thicker gold film on top of a PDMS stamp with columnar features. In this case, the gold film is rapidly sputtered onto the PDMS stamp to deliberately induce wrinkles on the surface. After vapor swelling, the gold along the columns is stretched to smooth the wrinkles, while the metal film perpendicular to the column tends to fracture, and cracks occur at the edge of each column owing to stress concentration. After transfer printing, the gold metal is transferred onto another flat substrate with nanoscale gaps; it is noteworthy that the column features on as-used PDMS stamp are very shallow so that the metal on the trench of stamp can also be transferred upon swelling.

Figure 2 shows a set of scanning electron microscopy (SEM) images of as-prepared metal films with tunable nanogaps. As shown in Figure 2a, the Au film has wavelike wrinkles perpendicular to the column feature of PDMS stamp because of the buckling of metal film upon thermal effect[26b] during rapid sputtering. After treating the PDMS stamp in organic vapor and transferring the metal to another substrate, the metal film cracks. Nanogaps form along the columns while the wrinkles are stretched smooth, as indicated in Figure 2b. Figure 2c–f shows large-area SEM images of nanogaps in Au metal with different gap widths. To get controllable and reproducible nanogap sizes, the PDMS stamp is first swelled in an organic vapor with higher swelling ratio S, such as chloroform. With such swelling agents, the gap between two adjacent metal films can reach several micrometers, and the metal films are completely separated. Then, the PDMS stamp is treated with an organic vapor with lower S, such as acetone or methanol, where the gap can be withdrawn into several hundreds or tens of nanometers, as indicated in Figure 2d–f. The easily fabricated large-area nanogap arrays with tunable width and spacing between nanogaps should find broad applications in reconfigurable protein matrices, collective excitations of the conduction electrons, single molecular detection, or nanogap electrodes in the near future.

Figure 3 shows the tunable cracking of an ultrathin metal film and its transfer printing to give microarrays of metallic nanoparticles. The SEM images in Figure 3a–d show the original PDMS stamp, the transferred metal microarrays after organic vapor swelling, the magnified view

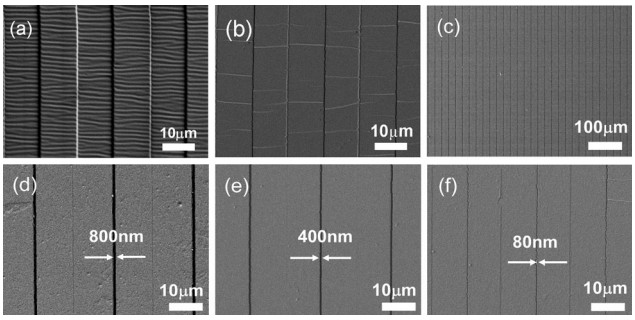

Figure 2. SEM images of metal film with nanogaps after vapor swelling. a) The original PDMS stamp with sputtered Au film (18 nm). b, c) nanogaps on Au film transferred from PDMS after swelling. d–f) PDMS swelled in chloroform vapor ($S = 1.39$) for about 3 h, then moved into different solvent vapors for different periods of time: d) acetone ($S = 1.06$, 3 h), e) methanol ($S = 1.02$, 15 min), f) methanol (30 min). S = swelling ratio.

of the metal nanostructures, and metal nanostructures from swelling with vapors with higher S factor, respectively. The atomic force microscopy (AFM) images in Figure 3e, f show the thickness of the metal thin film and the mean diameter of as-prepared nanoparticles to be 9 and 80 nm, respectively. The nanostructures in both Figure 2 and Figure 3 can be fabricated with great reproducibility as long as the organic vapor is carefully selected and its concentration carefully controlled.

It is well-established that noble-metal nanoparticles, in particular Au and Ag, support plasmon resonances that can be tuned throughout the UV/Vis/NIR region.[27] Therefore, UV/Vis absorption spectra are used herein to characterize the finer controllability of as-prepared metallic nanostructures. Figure 3g shows the UV/Vis spectra of Au nanoparticle arrays under different organic vapors, and Figure 3h shows the Au nanostructures fabricated under organic vapors with different mixture ratios. The results in Figure 3g, h clearly show that the size and spacing of as-prepared metallic nanoparticles can be effectively tuned with organic vapors and their mixtures;

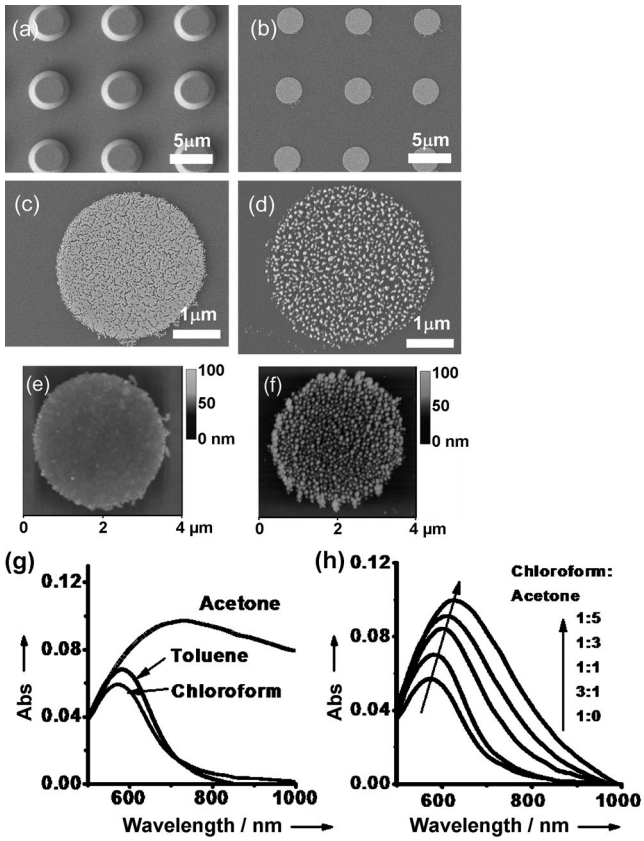

Figure 3. SEM (a–d) and AFM images (e,f) of metal thin film with nanoparticle shape after vapor swelling, and their UV/Vis spectra arising from plasmonic adsorption (g,h). a) The original PDMS stamp with sputtered Au film (9 nm). b) Au nanostructures transferred from PDMS after treatment with organic vapor. c) The cracked Au thin film after swelling of the PDMS stamp with acetone. d) The cracked Au thin film after swelling with chloroform, showing smaller nanoparticles with more space between them. e) The Au film transferred directly from PDMS stamp. f) AFM image of the film in (d). g,h) UV/Vis absorption spectra obtained from the Au nanostructures produced in the designated conditions.

moreover, the results also indicate that the facile fabrication approach is capable of producing well-ordered and highly regulable surface plasmons.

Figure 4 shows the transfer printing of metal nanostructures onto flexible plastic substrate as not only a patterning method but also a metal-enhanced fluorescence factor in the manufacturing of organic light-emitting diodes (OLEDs).[28] Comparing with shadow-mask processes, laser- or lamp-induced forward transfer, cold welding, and other techniques in patterning of metal electrodes for OLEDs, the transfer printing process described herein can directly and precisely print

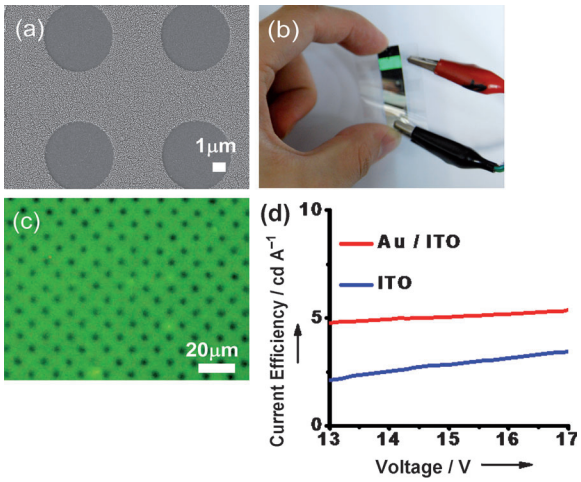

Figure 4. a) SEM image of the as-prepared Au nanostructures (except circular area). b) Digital photograph of OLEDs fabricated on flexible plastic substrate (indium tin oxide (ITO) on poly(ethylene terephthalate) (PET)), with Au nanostructures on ITO. c) Magnification of (b). d) Current efficiencies as a function of voltage.

metal nanostructures onto desired areas, as shown in Figure 4a–c. The efficiencies of OLEDs made from patterned metal nanostructures are obviously better than those of bare ITO electrodes (Figure 4d) because the surface plasmons of the patterned area cause a metal-enhanced fluorescence effect (in our design, the factor is about 1.2) by concentrating light through subwavelength nanostructures.[29]

Noble-metal nanostructures can produce highly magnified local electromagnetic fields when they are coupled with light, and the enhancement in local field and strong scattering is also very useful for surface-enhanced Raman scattering (SERS) and thus for chemical sensors or biosensors. Figure 5 shows the SERS spectra of rhodamine B on silicon wafer with Au nanostructures transfer-printed from organic-vapor-swelled PDMS stamp. From Figure 5a, we clearly see that the SERS effect of Rhodamine B (R6G) is much stronger on metal nanostructures than on flat gold thin film. Through a silver staining enhancement method to construct a silver–gold conjugated system based on the metal nanostructures, the

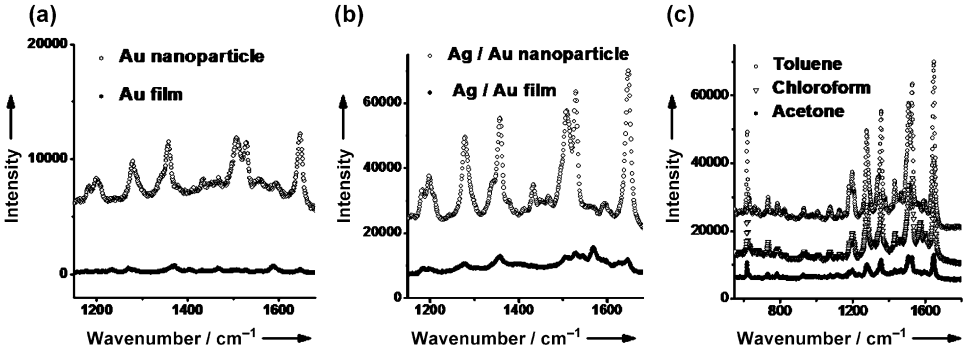

Figure 5. SERS spectra obtained from the nanostructures produced as the condition in the chart. The concentration of R6G for filled and open symbols in (a) is 0.5×10^{-6} M and 0.5×10^{-8} M, respectively, in (b) is 10^{-7} M and 10^{-9} M, and in (c) for all curves is 10^{-9} M. Silver staining time 6 min (b,c). The SERS enhancement factor (top to bottom in each case) is about 2×10^{2}, 0.9×10^{5} (a), 2.2×10^{4}, 3×10^{7} (b), and 0.4×10^{7}, 1.5×10^{7}, 3×10^{7} (c).

SERS effect shows even bigger differences with much lower dye concention, (shown in Figure 5b). Similar to the results in Figure 3 and Figure 4, the tunable cracking of metallic thin films under different organic vapor can induce a controllable SERS effect with high sensitivity towards different compounds. It is noteworthy that the metal nanoparticles produced under chloroform have bigger spaces in between than under toluene vapor, while the SERS effects show that metal nanostructures produced from swelling with toluene give the strongest signal; we speculate that the "hot spot" among metal nanoparticles varies under different organic vapors, and Au nanostructures produced under tolune vapor happen to induce suitable "hot spots" and thus the strongest SERS effect.

In summary, we demonstrate herein a very simple and inexpensive procedure for fabricating metallic nanostructures. Metallic nanostructures such as nanoparticles and nanogaps can be achieved by means of thin metal film deposition on a PDMS stamp, with subsequent organic vapor swelling of the stamp to induce the tunable cracking of the metal film, and transfer printing of the metal nanostructures in the final patterning step. The plasmonic effect of as-prepared metal nanostructures has been demonstrated by UV/Vis spectroscopy and applications in OLEDs and SERS. All of these effects show high degrees of tunability and controllability. The organic-vapor-induced metal nanostructures have essential merits such as room-temperature preparation, conformal contact printing, tunable particle size and spacing, large-area fabrication, and high-resolution patterning. These advantages make the nanofabrication approach very useful in manufacturing next-generation optoelectronic devices, especially flexible and stretchable organic electronics, where conventional patterning methods are generally not applicable.

Experimental Section

All materials and chemicals are commercially available and were used as received. Silver enhancer solution was purchased from Aldrich. Rhodamine B (R6G) and 3-mercaptopropyltrimethoxysilane were purchased from Alfa Aesar, ITO/PET with a sheet resistance less than 35 $\Omega\,\square^{-1}$ was purchased from Zhuhai Kaivo Electronic Components Co., Ltd. All other reagents were purchased from Sinopharm Chemical Reagent Beijing Co. All the SEM images were recorded with a JEOL 7401 microscope, and the AFM images were recorded using a Veeco D3100 instrument. Absorption spectra were acquired using a Cary 50 Probe UV/Vis spectrophotometer. The luminance–current–voltage characteristics were measured using a Keithley 4200 semiconductor characterization system. Optical images were recorded with a Nikon TE2000-U optical microscope. SERS spectra were measured by Renishaw inVia microscope.

Fabrication of metal nanostructures on silicon wafer: Soft lithography and rapid prototyping were used to fabricate features in SU-8 (Micro-Chem Corp.), which were subsequently replica-molded using a PDMS prepolymer to fabricate the flexible stamps. The stamps were coated with 8–25 nm thick layer of Au using a magnetic sputtering evaporation device (Techno Corp., Beijing). Silicon wafers were treated with 30% H_2O_2/70% H_2SO_4 and washed with deionized water and then coated 3-mercaptopropyltrimethoxysilane in ethanol. The Au-coated PDMS was placed in a sealed chamber full of organic vapor for swelling. Afterwards, the swelled PDMS stamp and SAM-treated silicon wafer were brought into conformal contact and separated to obtain metal nanostructures on Si wafer.

OLED fabrication and measurements: Patterned ITO/PET was obtained by etching in HCl for 45 s. ITO/PET substrates were cleaned successively by ultrasonication in diluted dishwashing detergent, water, de-ionized water, and alcohol, and then dried for 2 h before use. Metal nanoparticles were transferred onto SAM-ITO coated with 3-mercaptopropyltrimethoxysilane. The doped emitting layers were obtained by co-evaporating NPB and Alq_3 (NPB = *N*,*N*′-bis(1-naphthyl)-*N*,*N*′-diphenyl-1,1′-biphenyl-4,4′-diamine, Alq3 = tris(8-quinolinolate)aluminum). The device structure is anode/NPB (50 nm)/Alq_3 (50 nm)/Mg:Ag (10:1) (150 nm)/Ag (50 nm). The emitting areas were defined by a mask with $3\times3\ mm^2$ patterns for measurement and $5\times5\ mm^2$ for image. All the measurements were carried out in air at room temperature without encapsulation.

SERS measurements: Ag-capped Au nanostructures on Si wafer can be obtained by sequential silver staining of Au nanostructures. In brief, silver enhancer solution A, solution B, and water were mixed in a volume ratio of 1:1:2 immediately before use and applied to the Si wafer with the Au nanostructures. After 2–10 min, the substrate was rinsed with water for use. For SERS measurements, 10 μL R6G solution at different concentrations was dispersed on the substrates; the samples were dried in nitrogen to evaporate any moisture. A HeNe laser (633 nm) was used as the light source for the excitation.

Received: September 13, 2011
Published online: November 3, 2011

Keywords: nanofabrication · nanostructures · soft lithography · surface plasmon resonance · thin films

[1] K. Jasuja, V. Berry, *ACS Nano* **2009**, *3*, 2358.
[2] A. Sassolas, B. D. Leca-Bouvier, L. J. Blum, *Chem. Rev.* **2008**, *108*, 109.
[3] H. J. Chen, T. Ming, L. Zhao, F. Wang, L.-D. Sun, J. F. Wang, C.-H. Yan, *Nano Today* **2010**, *5*, 494.
[4] N. Zettsu, J. M. McLellan, B. Wiley, Y. D. Yin, Z.-Y. Li, Y. N. Xia, *Angew. Chem.* **2006**, *118*, 1310; *Angew. Chem. Int. Ed.* **2006**, *45*, 1288.
[5] E. J. Menke, M. A. Thompson, C. Xiang, L. C. Yang, R. M. Penner, *Nat. Mater.* **2006**, *5*, 914.
[6] Y. N. Xia, J. A. Rogers, K. E. Paul, G. M. Whitesides, *Chem. Rev.* **1999**, *99*, 1823.
[7] Z. Fan, H. Razavi, J.-W. Do, A. Moriwaki, O. Ergen, Y.-L. Chueh, P. W. Leu, J. C. Ho, T. Takahashi, L. A. Reichertz, S. Neale, K. Yu, M. Wu, J. W. Ager, A. Javey, *Nat. Mater.* **2009**, *8*, 648.
[8] Y. N. Xia, G. M. Whitesides, *Angew. Chem.* **1998**, *110*, 568; *Angew. Chem. Int. Ed.* **1998**, *37*, 550.
[9] A. Perl, D. N. Reinhoudt, J. Huskens, *Adv. Mater.* **2009**, *21*, 2257.
[10] J. A. Rogers, Z. N. Bao, K. Baldwin, A. Dodabalapur, B. Crone, V. R. Raju, V. Kuck, H. Katz, K. Amundson, J. Ewing, P. Drzaic, *Proc. Natl. Acad. Sci. USA* **2001**, *98*, 4835.
[11] Y.-L. Loo, R. L. Willett, K. W. Baldwin, J. A. Rogers, *J. Am. Chem. Soc.* **2002**, *124*, 7654.
[12] J. C. Love, L. A. Estroff, J. K. Kriebel, R. G. Nuzzo, G. M. Whitesides, *Chem. Rev.* **2005**, *105*, 1103.
[13] A. C. von Philipsborn, S. Lang, A. Bernard, J. Loeschinger, C. David, D. Lehnert, M. Bastmeyer, F. Bonhoeffer, *Nat. Protoc.* **2006**, *1*, 1322.
[14] S. A. Lange, V. Benes, D. P. Kern, J. K. H. Hörber, A. Bernard, *Anal. Chem.* **2004**, *76*, 1641.
[15] A. L. Briseno, S. C. B. Mannsfeld, M. M. Ling, S. Liu, R. J. Tseng, C. Reese, M. E. Roberts, Y. Yang, F. Wudl, Z. N. Bao, *Nature* **2006**, *444*, 913.

[16] E. Menard, M. A. Meitl, Y. Sun, J.-U. Park, D. J.-L. Shir, Y.-S. Nam, S. Jeon, J. A. Rogers, *Chem. Rev.* **2007**, *107*, 1117.
[17] M. Geissler, J. M. McLellan, Y. N. Xia, *Nano Lett.* **2005**, *5*, 31.
[18] M. Q. Xue, Y. L. Yang, T. B. Cao, *Adv. Mater.* **2008**, *20*, 596.
[19] M. M. Alkaisi, R. J. Blaikie, S. J. McNab, R. Cheung, D. R. S. Cumming, *Appl. Phys. Lett.* **1999**, *75*, 3560.
[20] T. Ito, S. Okazaki, *Nature* **2000**, *406*, 1027.
[21] Q. Xu, R. M. Rioux, M. D. Dickey, G. M. Whitesides, *Acc. Chem. Res.* **2008**, *41*, 1566.
[22] D. J. Lipomi, R. V. Martinez, G. M. Whitesides, *Angew. Chem.* **2011**, *123*, 8720; *Angew. Chem. Int. Ed.* **2011**, *50*, 8566.
[23] X. Yan, J. M. Yao, G. Lu, X. Li, J. H. Zhang, K. Han, B. Yang, *J. Am. Chem. Soc.* **2005**, *127*, 7688.
[24] D.-Y. Wu, J.-F. Li, B. Ren, Z.-Q. Tian, *Chem. Soc. Rev.* **2008**, *37*, 1025.
[25] C. X. Ji, P. C. Searson, *J. Phys. Chem. B* **2003**, *107*, 4494.
[26] a) H. A. Atwater, A. Polman, *Nat. Mater.* **2010**, *9*, 205; b) F. F. Wang, M. Q. Xue, T. B. Cao, *Adv. Mater.* **2009**, *21*, 2211.
[27] G. H. Chan, J. Zhao, E. M. Hicks, G. C. Schatz, R. P. V. Duyne, *Nano Lett.* **2007**, *7*, 1947.
[28] R. Bardhan, N. K. Grady, J. R. Cole, A. Joshi, N. J. Halas, *ACS Nano* **2009**, *3*, 744.
[29] A. Fujiki, T. Uemura, N. Zettsu, M. Akai-Kasaya, A. Saito, Y. Kuwahara, *Appl. Phys. Lett.* **2010**, *96*, 043307.

